KN.1.7.1

HIGH ACCURACY STEADY STATE SIMULATION MODEL AND SIMULATOR FOR HVAC SYSTEMS

Kiyoshi Saito, Prof., Waseda University, 3-4-1, Okubo, Sinjuku, Tokyo, Japan
Keisuke Ohno, Research associate, Waseda University, 3-4-1, Okubo, Sinjuku, Tokyo, Japan

Abstract: Recently, the year-round performance of heating, ventilating, and air-conditioning (HVAC) systems has been greatly enhanced. A major reason for this improvement is the introduction of the seasonal performance factor (SPF) for rating systems, which has replaced the coefficient of performance..
There is a demand for manufacturers to improve the SPF; thus, a high-precision simulation technique must be established to evaluate system performance under various driving conditions throughout the year. Accordingly, high-precision mathematical models of a CO_2 heat pump water heater, a desiccant air-conditioning system, a hybrid air-conditioning system for a data center, and an absorption heat transformer were developed, and their validity was experimentally investigated. A simulator called "Energy flow +M" was also developed to easily calculate the performance of HVAC systems, based on the modular analysis theory suggested by the authors and the mathematical model that we developed.
In this study, the mathematical models of the above systems were validated using an experiment with an actual machine. Furthermore, it was verified that we could easily calculate the performance of HVAC systems with our simulator using a graphical user interface.

Key Words: simulation, mathematical model, air-conditioning, refrigeration, heating

1 INTRODUCTION

The performance of heating, ventilating, and air-conditioning (HVAC) systems under a variety of operating conditions throughout the year has been greatly enhanced through the use of various innovative components and methods. One of the factors in this enhancement is the use of the seasonal performance factor (SPF) for rating systems, instead of the coefficient of performance (COP); there is a demand for manufacturers to improve the SPF.
There have been many new types of refrigerants, heat exchangers, and compressors developed, and it is necessary to quickly evaluate the performance of a system when these are adopted for an actual machine. It is also necessary to find methods to easily examine the potential of various systems such as compression- or absorption-type heat pumps and dehumidification air-conditioning systems. Thus, the establishment of a high-precision simulation technique for a wide range of driving conditions is essential because the SPF should be investigated under a variety of driving conditions.
Therefore, in this study, a high-precision mathematical model was developed, and the validity of the model was investigated using a wide range of experiments. We especially focused on the mathematical modes of a CO_2 heat pump water heater, a desiccant air-conditioning system, a hybrid air-conditioning system for a data center, and an absorption heat transformer. Furthermore, a simulator called "Energy flow +M" was developed, based on the modular analysis theory that the authors suggested. This simulator uses the mathematical models that we developed and makes numerical calculations possible.

2 CO_2 HEAT PUMP WATER HEATER

2.1 System Description

A CO_2 heat pump water heater is a compression-type heat pump system that is used to heat water. This system uses CO_2 as a refrigerant. CO_2 is sometimes regarded as a greenhouse gas. However, as a refrigerant, CO_2 is far better than the chlorofluorocarbons (CFCs) that are commonly used because the global warming potential of CO_2 is far lower than those of CFCs. A feature of this system is its use of the super critical region of the fluid, which increases the pressure excessively. However, for a water heater, the supercritical region is very effective at enhancing the efficiency of the system. This is why the market for CO_2 heat pumps is increasing, especially in Japan. The flow and a photo of the actual system are shown in Figure 1.

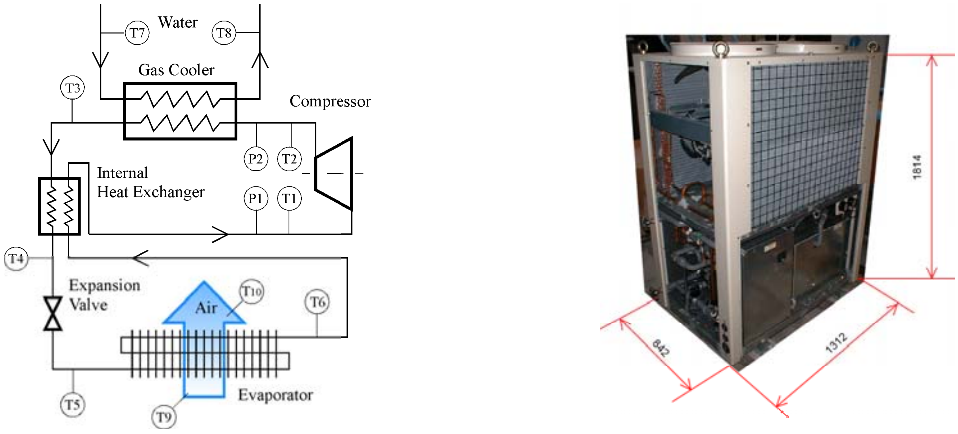

FIGURE 1: Schematic Flow and Photo of CO_2 Heat Pump Water Heater

2.2 Mathematical Model

Because of the page limitation, only the gas cooler model is shown. The authors show the model details in another paper (Kato 2008). The gas cooler is a helical-type heat exchanger, where water flows outside the inner tube, and refrigerant flows inside the inner tube.
The refrigerant continuity, energy, and pressure drop are as follows.

$$\frac{\mathrm{d}}{\mathrm{d}z_r}(\rho_r u_r) = 0 \tag{1}$$

$$\frac{\mathrm{d}}{\mathrm{d}z_r}\left(\rho_r u_r \frac{\pi d_{i,i}{}^2}{4} h_r\right) = -q_i \tag{2}$$

$$\frac{\mathrm{d}P_r}{\mathrm{d}z_r} = -f_{r,H}\frac{1}{d_{i,i}}\frac{\rho_r u_r{}^2}{2} \tag{3}$$

The hot water continuity, energy, and pressure drop are as follows.

$$\frac{\mathrm{d}}{\mathrm{d}z_w}(\rho_w u_w) = 0 \tag{4}$$

$$\frac{\mathrm{d}}{\mathrm{d}z_w}\left[\rho_w u_w \left(\frac{\pi d_{o,i}{}^2}{4} - \frac{\pi d_{i,o}{}^2}{4}\right) h_w\right] = q_i \tag{5}$$

$$\frac{\mathrm{d}P_w}{\mathrm{d}z_w} = -f_{w,H}\frac{1}{d_{hyd}}\frac{\rho_w u_w{}^2}{2} \tag{6}$$

The heat transfer rate is derived from the following equations.

$$q_i = K_i \pi d_{i,i}(T_r - T_w) \tag{7}$$

$$\frac{1}{K_i \pi d_{i,i}} = \frac{1}{\xi_{gc}\cdot \alpha_i \pi d_{i,i}} + \frac{1}{2\pi\lambda_t}\ln\left(\frac{d_{i,o}}{d_{i,i}}\right) + \frac{1}{\alpha_o \pi d_{i,o}} \tag{8}$$

Here, ξ is the degradation factor by the oil contamination. Other researchers have shown that the effect is small when the tube size is larger than 4.0 mm. Therefore, we adopt 1.0 for ξ.

The heat transfer performance and friction factor of the refrigerant side are as follows.

$$\mathrm{Nu}_r = \frac{\left(f_{r,H}/8\right)\left(\mathrm{Re}_b - 1000\right)\mathrm{Pr}}{1.07 + 12.7\sqrt{f_{r,H}/8}\left(\mathrm{Pr}^{2/3} - 1\right)} \tag{9}$$

$$f_{r,H} = f_{r,S}\left\{\mathrm{Re}_f\left(\frac{d_{i,i}}{D_H}\right)^2\right\}^{0.05} \tag{10}$$

$$f_{r,S} = \left[1.82\log\left(\mathrm{Re}_f\right) - 1.64\right]^{-2} \tag{11}$$

The heat transfer performance and friction factor of the hot water side are as follows.

$$\mathrm{Nu}_w = \left\{0.65\,\mathrm{Re}_w^{1/2}\left(\frac{d_{hyd}}{D_H}\right)^{1/4} + 0.76\right\}\mathrm{Pr}_w^{0.175} \tag{12}$$

$$f_{w,H} = f_{w,S}\left\{\mathrm{Re}_w\left(\frac{d_{o,i}}{D_H}\right)^2\right\}^{0.05} \tag{13}$$

$$f_{w,S} = \frac{64}{\mathrm{Re}_w} \tag{14}$$

For the evaporator and internal heat exchanger, the heat transfer coefficient, which depends on the two-phase flow pattern of the refrigerant, is considered in detail. For the compressor, the isentropic and volumetric efficiencies are derived based on the results of an experiment.

2.3 Simulation and Experimental Results

Simulation and experimental results are shown in Figure 2. As can be seen, the simulation results agree very well with the experimental ones. Therefore, we confirmed the validity of our model.

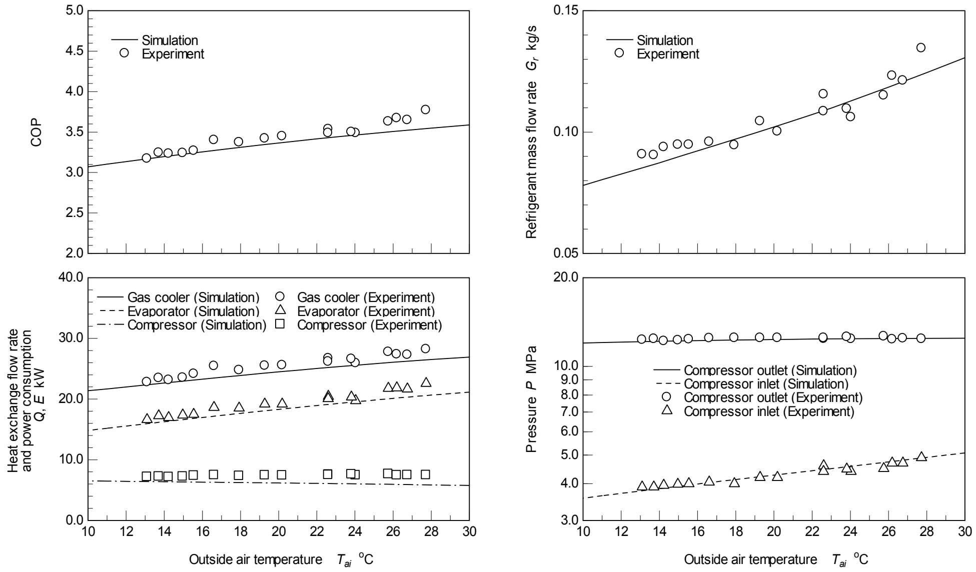

Figure 2: Simulation and Experimental Results for CO_2 Heat Pump Water Heater

3 DESICCANT AIR-CONDITIONING SYSTEM

3.1 System Description

A typical desiccant air-conditioning system is shown in Figure 3. This system consists of a desiccant wheel, cooler, heater, and sensible heat exchanger. The desiccant wheel is the main component in the desiccant air-conditioning system.

The process air is dehumidified by the desiccant wheel and then supplied to the space. The regeneration air removes the water from the desiccant wheel. Therefore, there are two air streams in the desiccant wheel.

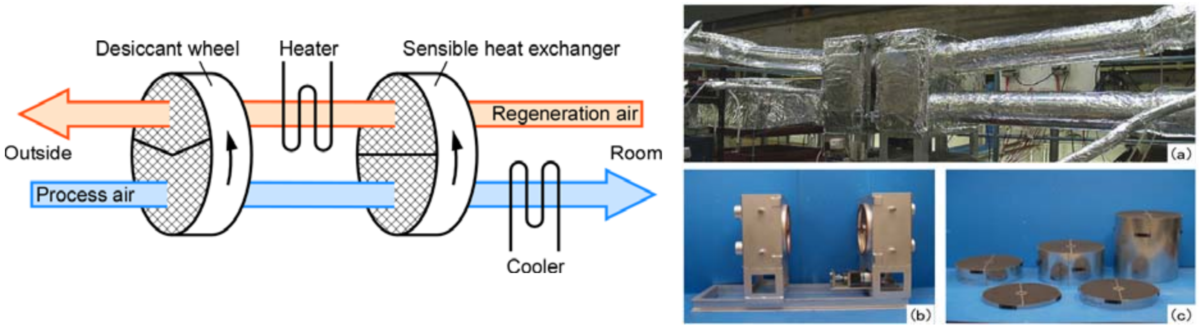

Figure 3: Schematic Flow and Photo of Desiccant Air-conditioning System

3.2 Mathematical Model

The desiccant wheel model can be explained as follows, with the details provided in a previous paper (Yamaguchi 2010). The desiccant wheel is a porous solid. The governing equations are developed by considering the heat and mass diffusion inside this porous solid. The mass diffusion equation of the water vapor in the pores is as follows:

$$\varepsilon\frac{\partial}{\partial t}(\rho_a w_a)+\nabla\cdot\mathbf{j}_p=\dot{m} \tag{15}$$

where $\dot{m}$ is the amount of desorbed water per unit volume from the solid surface to the pores, and $\boldsymbol{j}_p$ is the mass flux caused by the pore diffusion and is given by

$$\mathbf{j}_p=-\frac{\varepsilon D_p}{\tau_p}\nabla(\rho_a w_a) \tag{16}$$

The mass diffusion equation of the adsorbed water on the solid surface is as follows:

$$(1-\varepsilon)\frac{\partial}{\partial t}(\rho_d\omega_d)+\nabla\cdot\mathbf{j}_s=-\dot{m} \tag{17}$$

where $\boldsymbol{j}_s$ is the mass flux caused by the surface diffusion and is given by

$$\mathbf{j}_s=-\frac{(1-\varepsilon)D_s}{\tau_s}\nabla(\rho_d\omega_d)\,. \tag{18}$$

Because the continuum and Knudsen diffusions are considered to occur in series, the pore diffusivity is expressed as follows:

$$\frac{1}{D_p}=\frac{1}{D_m}+\frac{1}{D_K} \tag{19}$$

For the continuum diffusivity of the water vapor in the humid air,

$$D_m=\frac{0.926\times10^{-3}}{p_t}\left(\frac{T_a^{2.5}}{T_a+245}\right). \tag{20}$$

For the Knudsen diffusivity in pore with a mean pore radius of γ,

$$D_k=97\gamma\left(\frac{T_a}{M_w}\right)^{1/2}. \tag{21}$$

For the surface diffusivity,

$$D_s=1.6\times10^{-6}\exp\left(-0.45\frac{h_{ads}}{R_w T_d}\right). \tag{22}$$

The heat conduction equation of the humid air in the pores is as follows:

$$\varepsilon\frac{\partial}{\partial t}(\rho_a h_a)+\nabla\cdot\mathbf{q}_p+(\nabla\cdot\mathbf{j}_p)h_v=\dot{Q}+\dot{m}h_v \tag{23}$$

where $\dot{Q}$ is the sensible heat flow per unit volume from the solid to the humid air in the pores, and $\boldsymbol{q}_p$ is the heat flux caused by the heat conduction in the pores and is given by

$$\mathbf{q}_p = -\frac{\varepsilon k_a}{\tau_p}\nabla T_a \,. \tag{24}$$

The heat conduction equation for the solid and adsorbed water is as follows:

$$(1-\varepsilon)\frac{\partial}{\partial t}(\rho_d h_d) + \nabla\cdot\mathbf{q}_{sw} + (\nabla\cdot\mathbf{j}_s)h_w = -\dot{Q} - \dot{m}h_{ads} - \dot{m}h_w \,, \tag{25}$$

where $\boldsymbol{q}_{\mathrm{sw}}$ is the heat flux caused by the heat conduction in the solid and adsorbed water and is given by

$$\mathbf{q}_s = -\frac{(1-\varepsilon)k_{sw}}{\tau_s}\nabla T_d \,. \tag{26}$$

Next, the governing equations inside the air channel are developed. In the air channel, the mass conservation equation of the humid air is as follows:

$$\frac{\partial\rho_{ac}}{\partial t} + \frac{\partial\rho_{ac}u_{ac}}{\partial z} = \left(\frac{4}{d_h}\right) j_c \,. \tag{27}$$

The mass conservation of water vapor in humid air is as follows:

$$\frac{\partial\rho_{ac}w_{ac}}{\partial t} + \frac{\partial\rho_{ac}w_{ac}u_{ac}}{\partial z} = \left(\frac{4}{d_h}\right) j_c \tag{28}$$

where $\boldsymbol{j}_{\mathrm{c}}$ is the convective mass flux of the water vapor from the interface to the humid air that flows in the air channel. The driving force of the convective mass transfer is the vapor mass fraction difference. The convective mass flux is given by

$$j_c = \rho_{ac}\beta\left(w_{ac,i} - w_{ac}\right) \tag{29}$$

The energy equation of the humid air is as follows:

$$\frac{\partial\rho_{ac}h_{ac}}{\partial t} + \frac{\partial\rho_{ac}h_{ac}u_{ac}}{\partial z} = \left(\frac{4}{d_h}\right)\left(q_c + j_c h_{vc}\right) \tag{30}$$

where $\boldsymbol{q}_{\mathrm{c}}$ is the convective sensible heat flux from the interface to the humid air that flows in the air channel. The driving force of the convective sensible heat transfer is the temperature difference. The convective sensible heat flux is given by

$$q_c = \alpha\left(T_{ac,i} - T_{ac}\right) \tag{31}$$

The pressure drop equation is calculated as the steady state as follows:

$$\frac{dp_{ac}}{dz} = -f\,\frac{\rho_{ac}u_{ac}^2}{2d_h} \tag{32}$$

To calculate the simulation model, the convective heat and mass transfer coefficients α and β and the friction factor of the air channel f have to be determined.

3.3 Simulation and Experimental Results

We carried out not only simulations but also detailed experiments. Figure 4 shows the simulation and experimental results. The results of the simulation and experiment agreed very well with each other. From this, we confirmed the validity of the model.

4 HYBRID AIR-CONDITIONING SYSTEM FOR DATA CENTER

4.1 System Description

In recent years, there has been a great demand to save electrical power in data centers. The air-conditioning system in a data center must be operated year round owing to the extremely large amount of heat rejection from IT devices. In order to decrease the year-round energy consumption, it is important to wisely use low temperature outdoor air during cool and cold seasons. To use this cold heat effectively, we developed a completely new package A/C system that combines a compression-type cycle and a free cooling one. In warm and hot seasons, this system adopts the normal compression-type cycle, without a refrigerant pump. In the cool and cold seasons, it adopts the free cooling cycle, in which a refrigerant pump is used to circulate the refrigerant instead of the compressor.

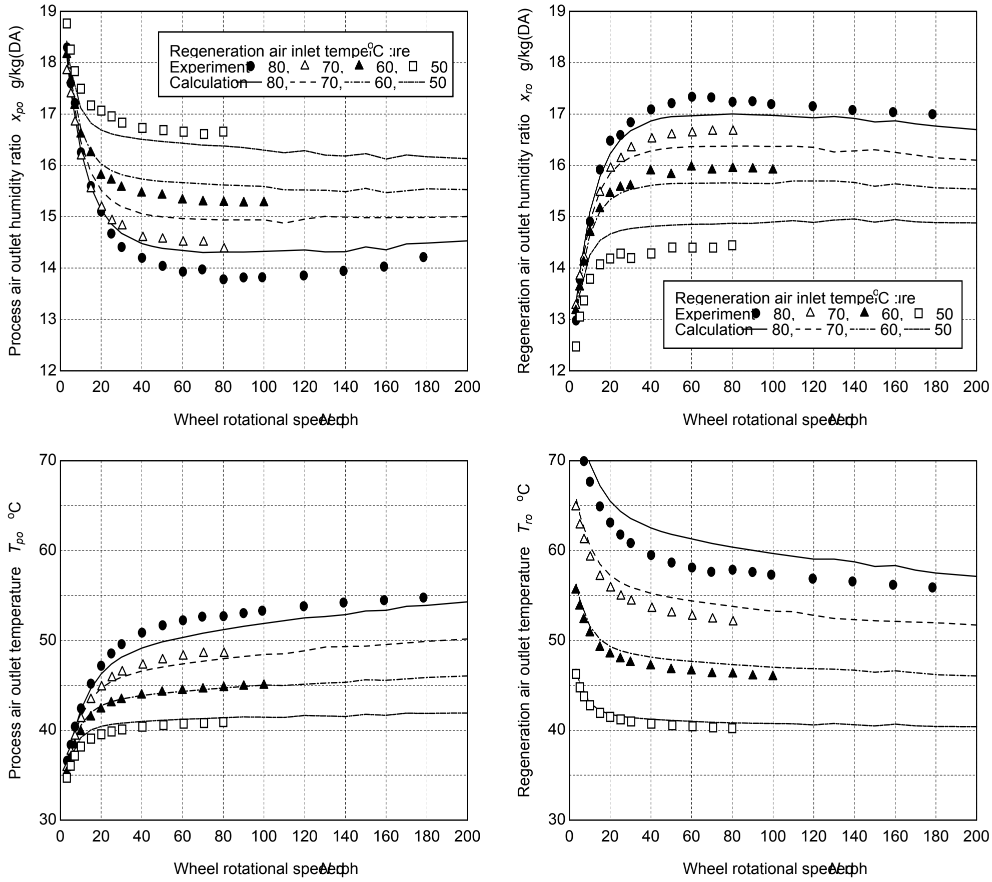

Figure 4: Simulation and experimental results of desiccant air-conditioning system

The new hybrid cycle and a photo of the actual system are shown in Figure 5. This cycle consists of two heat exchangers, an expansion valve, a compressor, a refrigerant pump, an accumulator, a receiver, and a sub-condenser, which is used to prevent cavitation in the refrigerant pump. In the compression cycle, it uses the compressor, and the refrigerant circulation follows the red dashed line. In the free cooling cycle, it uses the refrigerant pump, and the refrigerant circulation follows the blue dashed line

4.2 Mathematical Model

The heat exchanger model is introduced as an example. The evaporator and

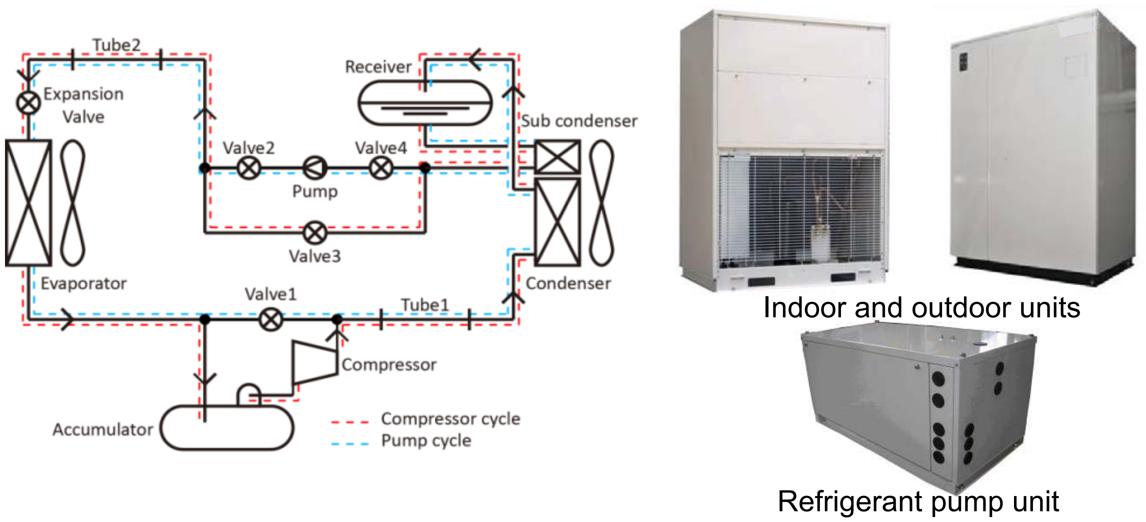

Figure 5: Schematic flow and photo of hybrid air-conditioning system for data center

condenser are treated using the same mathematical model.

The equation of continuity for the refrigerant, the pressure loss equation, and the equation of energy are as follows.

$$\frac{\partial \rho_{\mathrm{R}}}{\partial t}+\frac{\partial\left(\rho_{\mathrm{R}} v_{\mathrm{R}}\right)}{\partial z}=0 \tag{33}$$

$$\frac{\partial P_{\mathrm{R}}}{\partial z}=-f_{\mathrm{R}} \frac{2 \rho_{\mathrm{R}} v_{\mathrm{R}}^{2}}{D_{\mathrm{In}}} \tag{34}$$

$$\frac{\partial\left(\rho_{\mathrm{R}} u_{\mathrm{R}}\right)}{\partial t}+\frac{\partial\left(\rho_{\mathrm{R}} v_{\mathrm{R}} h_{\mathrm{R}}\right)}{\partial x}=-\frac{L c_{\mathrm{In}}}{S_{\mathrm{In}}} q_{\mathrm{In}} \tag{35}$$

The equation of energy for the tubes is as follows:

$$\rho_{\mathrm{M}} C_{\mathrm{M}} \frac{\partial T_{\mathrm{M}}}{\partial t}=\frac{L c_{\mathrm{In}}}{S_{\mathrm{M}}} q_{\mathrm{In}}-\left(q_{\mathrm{Out}}+j_{\mathrm{Out}} h_{\mathrm{VAP}}\right) \frac{A_{\mathrm{FC}}+\eta_{\mathrm{FIN}} A_{\mathrm{FIN}}}{S_{\mathrm{M}} L}. \tag{36}$$

The equation of continuity for the air, the pressure drop equation, and the equation of energy are as follows.

$$\rho_{\mathrm{A,O}} v_{\mathrm{A,O}} L_{\mathrm{A}}-\rho_{\mathrm{A,I}} v_{\mathrm{A,I}} L_{\mathrm{A}}=j_{\mathrm{Out}} \frac{A_{\mathrm{FC}}+\eta_{\mathrm{FIN}} A_{\mathrm{FIN}}}{L} \tag{37}$$

$$P_{\mathrm{A,O}}-P_{\mathrm{A,I}}=-f_{\mathrm{A}} \frac{2 L_{\mathrm{A2}} \rho_{\mathrm{A}} v_{\mathrm{AC}}^{2}}{D_{AC}} \tag{38}$$

$$\rho_{\mathrm{A,O}} v_{\mathrm{A,O}} X_{\mathrm{A,O}} L_{\mathrm{A}}-\rho_{\mathrm{A,I}} v_{\mathrm{A,I}} X_{\mathrm{A,I}} L_{\mathrm{A}}=j_{\mathrm{Out}} \frac{A_{\mathrm{FC}}+\eta_{\mathrm{FIN}} A_{\mathrm{FIN}}}{L} \tag{39}$$

$$\rho_{\mathrm{A,O}} v_{\mathrm{A,O}} h_{\mathrm{A,O}} L_{\mathrm{A}}-\rho_{\mathrm{A,I}} v_{\mathrm{A,I}} h_{\mathrm{A,I}} L_{\mathrm{A}}=\left(q_{\mathrm{Out}}+j_{\mathrm{Out}} h_{\mathrm{VAP}}\right) \frac{A_{\mathrm{FC}}+\eta_{\mathrm{FIN}} A_{\mathrm{FIN}}}{L} \tag{40}$$

When the air exit temperature reaches the dew point, the fluid mass flux j is calculated as follows so that the air exit temperature and the dew point are equal.

$$j_{\mathrm{Out}}=\begin{cases} 0 & T_{\mathrm{DP,A,O}}<T_{\mathrm{A,O}} \\ f\left(P_{\mathrm{A,O}}, h_{\mathrm{A,O}}, T_{\mathrm{DP,A,O}}\right) & T_{\mathrm{DP,A,O}}=T_{\mathrm{A,O}} \end{cases} \tag{41}$$

The heat transfers between the refrigerant, heat transfer tubes, and air are calculated using the following equations.

$$q_{\mathrm{In}}=\alpha_{\mathrm{In}}\left(T_{\mathrm{R}}-T_{\mathrm{M}}\right) \tag{42}$$

$$q_{\mathrm{Out}}=\alpha_{\mathrm{Out}} \frac{\left(T_{\mathrm{M}}-T_{\mathrm{A,I}}\right)-\left(T_{\mathrm{M}}-T_{\mathrm{A,O}}\right)}{\ln \frac{\left(T_{\mathrm{M}}-T_{\mathrm{A,I}}\right)}{\left(T_{\mathrm{M}}-T_{\mathrm{A,O}}\right)}} \tag{43}$$

The heat transfer coefficient and pressure drop are shown below. Because these are correlations for smooth tubes or plate-fins, we use the correction coefficient to account for the effects of internal tube grooves, tube bends, and fin slits. For a single-phase flow, we use the following equation for the heat transfer coefficient α_{In} in the pipe.

$$\alpha_{\mathrm{In}}=\mathrm{Nu}_{\mathrm{R}} \frac{\lambda_{\mathrm{R}}}{D_{\mathrm{In}}} \tag{44}$$

$$\mathrm{Nu}_{\mathrm{R,SP}}=0.023 \mathrm{Re}_{\mathrm{R}}^{0.8} \mathrm{Pr}_{\mathrm{R}}^{n} \tag{45}$$

For two-phase condensation, we use the equation formulated by (Nozu 1983):

$$\mathrm{Nu}_{\mathrm{R,f,TP}}=0.018\left(\mathrm{Re}_{\mathrm{R,L}} \sqrt{\frac{\rho_{\mathrm{R,L}}}{\rho_{\mathrm{R,v}}}}\right)^{0.9}\left(\frac{x_{\mathrm{R}}}{1-x_{\mathrm{R}}}\right)^{0.1 x_{\mathrm{R}}+0.8} \times\left(\mathrm{Pr}_{\mathrm{R,L}}+\frac{8 \times 10^{3}}{\mathrm{Re}_{\mathrm{R,L}}^{1.5}}\right)^{1/3}\left(1+\frac{C_{1} H}{\mathrm{Pr}_{\mathrm{R,L}}}-0.2 \frac{H_{\mathrm{v}}}{\mathrm{Pr}_{\mathrm{R,v}}}\right) \tag{46}$$

$$\mathrm{Nu}_{\mathrm{R,b,TP}}=0.725\left(\frac{Ga\,\mathrm{Pr}_{\mathrm{R,L}}}{H}\right)^{0.25} \times \frac{\left\{1+0.003 \sqrt{\mathrm{Pr}_{\mathrm{R,L}}} C_{3}^{\left(3.1-\frac{0.5}{\mathrm{Pr}_{\mathrm{R,L}}}\right)}\right\}^{0.3}}{\left(1+C_{2} C_{4}\right)^{0.25}}. \tag{47}$$

For two-phase evaporation, we use the equation formulated by Yoshida et al. (1983):

$$\frac{\alpha_{\mathrm{In,TP}}}{\alpha_{\mathrm{In,SP,L}}} = 3.7\left\{ Bo\times10^{4} + 0.23\left(Bo\times10^{4}\right)^{0.69}\left(\frac{1}{X_{\mathrm{tt}}}\right)^{2}\right\}^{0.44} . \tag{48}$$

For a single-phase flow, we use the Blasius equation for the pressure loss coefficient f_{R}.

$$f_{\mathrm{R,SP}} = 0.079\,\mathrm{Re}_{\mathrm{R}}^{-0.25} \tag{49}$$

For two-phase flow, we use the following equations (Chisholm 1967):

$$f_{\mathrm{R,TP}} = 0.079\,\mathrm{Re}_{\mathrm{R,L}}^{-0.25}\,\phi_{\mathrm{L}}^{2} \tag{50}$$

$$\phi_{\mathrm{L}}^{2} = 1 + \frac{20}{X_{\mathrm{tt}}} + X_{\mathrm{tt}}^{2} . \tag{51}$$

We use the equations formulated by (Seshimo 1987) for the heat transfer rate of the fins α_{Out} and the pressure drop coefficient f_{A},

$$\alpha_{\mathrm{Out}}\,\frac{D_{ec}}{\lambda_{\mathrm{A}}} = 2.1\left(\mathrm{Re}_{\mathrm{A}}\ \mathrm{Pr}_{\mathrm{A}}\,\frac{D_{ec}}{L_{\mathrm{A2}}}\right)^{0.38} \tag{52}$$

$$f_{\mathrm{A}}\,\frac{L_{\mathrm{A2}}}{D_{ec}} = 0.43 + 35.1\left(\mathrm{Re}_{\mathrm{A}}\,\frac{D_{ec}}{L_{\mathrm{A2}}}\right)^{-1.07} \tag{53}$$

For the fan power consumption, we performed experiments in advance and formulated the fan power consumption function as follows:

$$W_{\mathrm{FAN}} = f\left(n\right) \tag{54}$$

4.3 Simulation and Experimental Results

In addition to a simulation, we performed an experiment with a rated cooling capacity of 45.0 kW by using R410A as the refrigerant and changing the outdoor temperature. We compared the experimental results with those for a simulation of the compression cycle and free cooling cycle. In the simulation, various conditions such as the indoor temperature were the same as those of the experiment. Figure 6(a) shows the results for the compression cycle. Figure 6(b) shows the results for the free cooling cycle. As shown in the figure, the simulation and experimental results agreed very well with each other, which confirmed the validity of the simulation model.

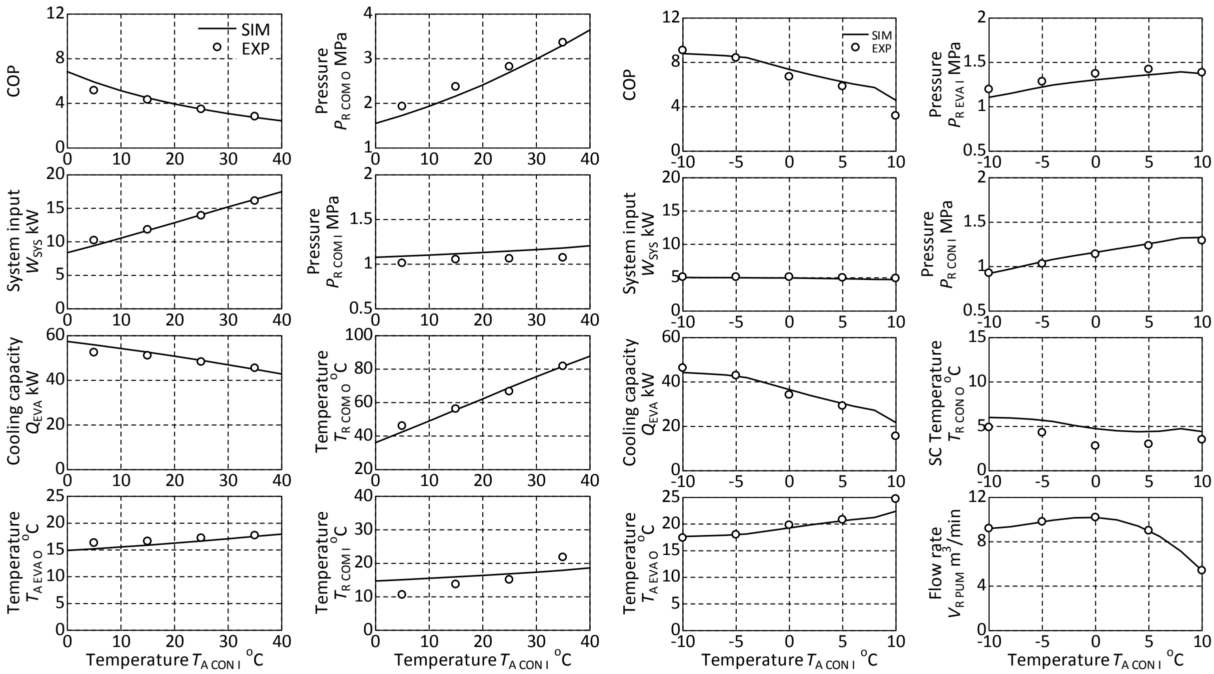

(a) Compression cycle **(b) Free cooling cycle**

Figure 6: Simulation and experimental results of hybrid air-conditioning system for data center

5 ABSORPTION HEAT TRANSFORMER

5.1 System Description

In this study, we investigated a two-stage absorption heat transformer, which could generate high temperature steam at approximately 180°C, driven by waste heat from hot water below 90°C. A model-scale (10 kW of steam) test apparatus and practical-scale (200 kW of steam) test apparatus were designed and built, and test operations were conducted.

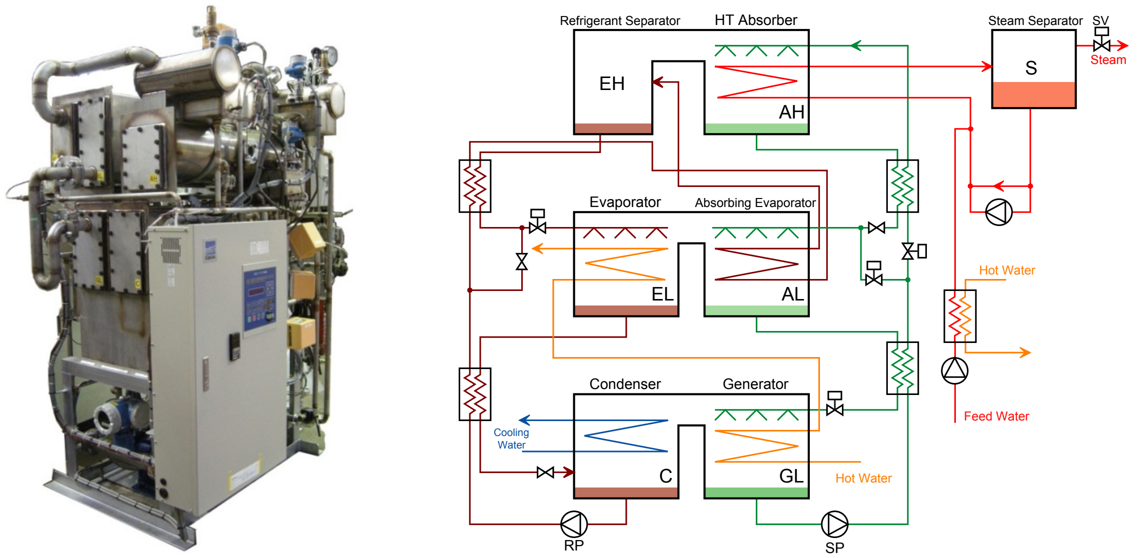

Figure 7: Schematic Flow and Photo of Double-stage Absorption Heat Transformer

5.2 Mathematical Model

Because of the page limitation, only the model of the absorber is shown here.

The continuity equation of the solution is

$$\frac{\partial \rho_S}{\partial t} + \frac{\partial \rho_S v_S}{\partial x} = \frac{j_{abs}}{\delta_S} \tag{55}$$

The continuity equation of LiBr is as follows:

$$\frac{\partial \rho_S X_S}{\partial t} + \frac{\partial \rho_S v_S X_S}{\partial x} = 0 \tag{56}$$

The energy equation of the solution is as follows:

$$\frac{\partial \rho_S u_S}{\partial t} + \frac{\partial \rho_S v_S h_S}{\partial x} = \frac{j_{abs} h_{abs} - q}{\delta_S} \tag{57}$$

The continuity equation of the cooling water is as follows:

$$\frac{\partial \rho_W}{\partial t} + \frac{\partial \rho_W v_W}{\partial x} = 0 \tag{58}$$

The continuity equation of the cooling water is as follows:

$$\frac{\partial \rho_W u_W}{\partial t} + \frac{\partial \rho_W v_W h_W}{\partial x} = \left(\frac{W}{S_W}\right) q \tag{59}$$

The continuity equation of the refrigerant vapor is as follows:

$$\frac{\partial \rho_V}{\partial t} V_V = G_{V,I} - j_{abs} A_{if} \tag{60}$$

The energy equation of the refrigerant vapor is as follows:

$$\frac{\partial \rho_V u_V}{\partial t} V_V = G_{V,I} h_{V,I} - j_{abs} h_{abs} A_{if} \tag{61}$$

The heat transfer rate is as follows:

$$q = K\left(T_S - T_W\right) \tag{62}$$

5.3 Simulation and Experimental Results

Figure 11 shows the results of experiments and simulations of the hot water temperature and mass flow rate parametric studies. For generated steam fixed at 180°C and inlet cooling water fixed at 25°C, increasing the temperature of the inlet hot water from 82°C to 94°C caused an increase in the refrigerant vapor from G and GL, i.e., the circulating refrigerant. The output from the high-stage absorber, i.e., generated steam, also increased. For generated steam fixed at 180°C and inlet cooling water fixed at 25°C, increasing the solution flow rate caused the concentration width of the cycle to narrow, and the COP to drop slightly.

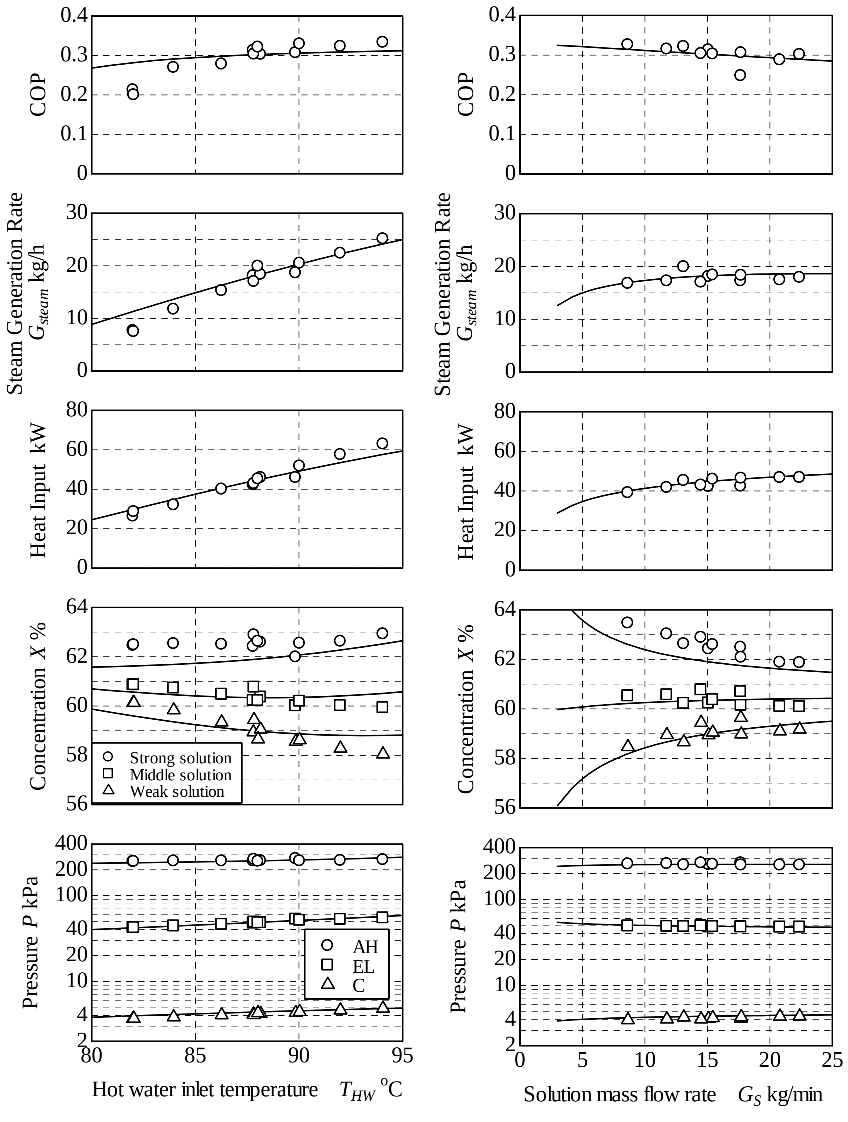

Figure 8: Simulation and Experimental Results for Double-stage Absorption Heat Transformer

6 DEVELOPMENT OF SIMULATOR

Modular analysis theory is a way to analyze the energy system with a unified method. Using this theory, we can develop a general-purpose analyzing simulator, as shown in Figure 9. This simulator is called “Energy flow + M”(Ohno 2010). With this simulator, a user can analyze a thermal system without mathematical procedures. Energy systems can be analyzed simply by connecting the graphical modules on the screen, as shown in Figure 9. Using this simulator reduces the burden imposed on the user to develop simulation code.

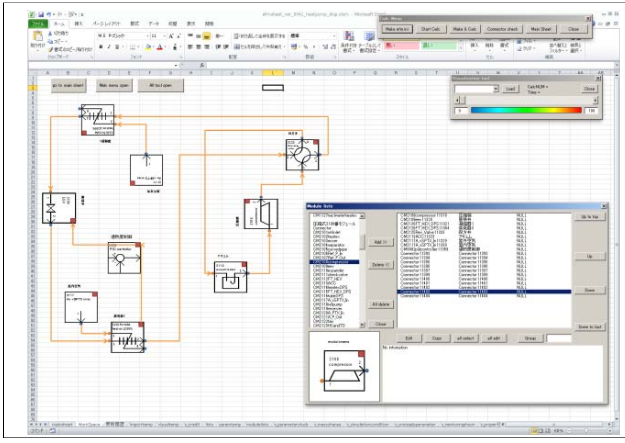

At present, the following systems can be calculated based on the modular analysis theory:
CO_2 heat pump water heater
Room air-conditioner
Variable refrigerant flow system
Absorption refrigerator, heat pump
Desiccant air-conditioning system
Solar thermal system

Figure 9: GUI of Simulator

7 CONCLUSIONS

In this paper, the mathematical models and simulation method for heating, refrigerating, and air-conditioning systems were introduced. We presented the simulation results for a CO_2 heat pump water heater, a desiccant air-conditioning system, a hybrid air-conditioning system for a data center, and an absorption heat transformer. We will introduce simulation results for other HVAC systems soon.

8 REFERENCES

Chisholm D., et al. 1967. “A theoretical basis for the Lockhart–Martinelli correlation for two-phase flow,” International Journal of Heat and Mass Transfer, Vol. 10, No. 12, pp. 1767–1778.

Inoue N., et al. 2005. “Analysis on characteristics of a boosted temperature type absorption heat pump,” Transactions of the Japan Society of Refrigerating and Air Conditioning Engineers, Vol. 22, No. 2, pp. 173–184 (in Japanese).

Kato D. 2008. “Static simulation and experiment of CO_2 heat pump water heater,” 8th IIR Gustav Lorentzen Conference on Natural Working Fluids, IIR.

Nozu S., et al. 1983. Refrigeration, Vol. 58, No. 669, pp. 659–668 (in Japanese).

Ohno K., K. Saito, Y. Udagawa, K. Sekiguchi, and M. Yanagi. 2012. “Study on packaged air conditioners with refrigerant pump for data centers (Part 2: parameter study),” Proceedings of the 2012 JSRAE Annual Conference, pp. 563–566.

Ohno K. and K. Saito. 2010. “Global unsteady state simulation of compression type heat pump with modular analysis,” ACRA, Tokyo.
Rivera W., et al. 1993. “Thermodynamic study of advanced absorption heat transformers - I. single and two stage configurations with heat exchangers,” Heat Recovery Systems & CHP, Vol. 14, No. 2, pp. 173–183.

Sekiguchi K., S. Waragai, T. Uekusa, and K. Yamasaki. 2010. “Development of a high-efficiency air cooled packaged air-conditioner for data centers,” ASHRAE Transactions, Vol. 116, No. 1, pp. 330–335.

Seshimo Y., et al. 1987. “Heat transfer and friction performance of plate fin and tube heat exchangers at low Reynolds numbers (1st report, characteristics of single-row),” Transactions of the Japan Society of Mechanical Engineers. B, Vol. 53, No. 486, pp. 581–586.

Tano H., et al. 2010. “Static simulation of multistage absorption heat transformer with modular analysis,” Proc. Of International Sorption Heat Pump Conference.

Udagawa Y., K. Sekiguchi, M. Yanagi, K. Saito, and K. Ohno. 2012. “Study on packaged air conditioners with refrigerant pump for data centers (Part 1: modeling and validity examination of the packaged air conditioners),” Proceedings of the 2012 JSRAE Annual Conference, pp. 559–562.

Udagawa Y., S. Waragai, M. Yanagi, and W. Fukumitsu. 2010. “Study on free cooling systems for data centers in Japan,” INTELEC, 12-4.

Yamaguchi S., K. Saito, et al. 2010. International Symposium on Innovative Materials for Processes in Energy Systems, Singapore.

Yoshida S., et al. 1983. Refrigeration, Vol. 58, No. 666, pp. 331–338 (in Japanese).

Ziegler F. and G. Alefeld. 1987. “Coefficient of performance of multistage absorption cycles,” International Journal of Refrigeration, Vol. 10, pp. 285–295.